A model for the exergy analysis of photosynthesis based on ancillary and satellite data on a Mediterranean mixed forest

Danilo Lombardi[a], Marcello Vitale[a], Enrico Sciubba[b]

[a] Department of Environmental Biology, Sapienza University of Roma, Roma 00185, Italy, danilo.lombardi@uniroma1.it, CA
[a] Department of Environmental Biology, Sapienza University of Roma, Roma 00185, Italy, marcello.vitale@uniroma1.it
[b] Department of Mechanical Engineering, UniCusano, Roma 00166, Italy enrico.sciubba@fondazione.uniroma1.it

Abstract:
Plant photosynthesis represents the primary pathway for the conversion of solar energy into chemical energy and is the fundamental driver of biospheric operation. Based on the classical thermodynamic analysis developed by Petela (2007) and Silva et al. (2015), who addressed photosynthesis as a highly irreversible, endothermic process and quantified its coupled radiative, thermal, and chemical energy exchanges, we propose here a slightly modified model that has the merit of making extensive use of non-local, real-time data (i.e., satellite and other aerial measurement devices).
A novelty of this study is its proposal to evaluate forest efficiency using exergy-based indicators: a lumped representation of photosynthesis is adopted and embedded within a detailed leaf energy balance model that treats the leaf as an energy converter. This allows for a consistent accounting of absorbed radiation, sensible and latent heat exchanges, and biochemical energy storage. A preliminary mass and energy balance is used to verify data consistency and agreement with literature values and field measurements. Energy and exergy terms are then compared to quantify irreversibility and assess differences between First- and Second Law descriptions. The exergy framework enables direct comparison among flows of different quality, provides a measure of irreversibility relative to primary resource use, and its procedures are compatible with industrial thermodynamic analyses, supporting sustainability-oriented assessments. The analysis spans a five-year period (2018–2022) and uses daily averaged datasets combining *in situ* eco-physiological measurements (CO_2 and H_2O fluxes, Leaf Area Index), remote sensing products (canopy albedo, surface temperature), and meteorological observations (radiation, air temperature, humidity, wind speed, precipitation).Two efficiency indicators are derived: first, a system-level exergy efficiency is calculated as the ratio of the useful output to the used input. The second one focuses on the photosynthetic engine, relating the chemical exergy stored in sugars and associated tissue water to the exergy inputs specific to the photosynthetic reactions.
These two indicators measure how the functional processes of a forest system vary in response to changing environmental conditions and provide key information to support the sustainable management of forest ecosystems.

Keywords:
Photosynthesis; Exergy Analysis, Remote Sensing Data, Forest Efficiency.

1. Introduction

Plant Photosynthesis (PPS) represents the primary pathway for the conversion of solar energy into chemical energy and is the fundamental driver of biospheric operation. Studying this process is important for several scientific and practical reasons:

a) PPS is the primary mechanism for the capture of solar radiation energy into the biosphere and is at the basis of nearly all food chains, directly through plants and algae and indirectly through organisms that consume them;
b) PPS is -strictly speaking- an endothermic chemical reaction that converts thermal radiation to chemical energy. The reaction (actually, the series of reactions) is inherently complex, and understanding the details of this process provides insight into energy transfer, storage, and conversion at the molecular level;
c) The process involves complex biochemical pathways, enzymes, and membrane systems. Studying photosynthesis deepens understanding of cellular processes, electron transport, and enzyme regulation;
d) Since PPS plays a central role in regulating atmospheric gases by absorbing CO_2 and releasing O_2, a better understanding of this process helps quantifying Earth's climate balance and lead to the definition of new strategies to mitigate climate change. Furthermore, PPS has a regulatory role on ecosystems' productivity, biodiversity, and nutrient cycles, and its understanding is essential for ecology, conservation, and environmental management;
e) Knowledge of PPS is also essential for improving crop productivity and food security;
f) PPS shaped the evolution of life through the oxygenation of Earth's atmosphere. Investigating it helps explain how early life forms evolved and adapted to changing environmental conditions;
g) Research on PPS has inspired artificial photosynthesis and solar energy technologies. Mimicking natural light-harvesting systems may lead to cleaner and more sustainable energy conversion systems.

Because PPS is tightly coupled to canopy energy and water exchanges, shifts in photosynthetic functioning can propagate to whole-canopy metabolism, affecting carbon gain, evapotranspiration, and ultimately the capacity of forests to cope with and recover from environmental stress. Disturbances and chronic stressors may impair ecosystem functioning by altering key processes (e.g., biogeochemical cycling), reducing productivity and biodiversity, and producing recognizable symptoms of ecosystem "dysfunction" [1]. In this sense, metabolism—and, in forests, photosynthesis as a primary driver of carbon and water fluxes—provides a mechanistically meaningful entry point for diagnosing functional status and stress responses. The "Vigour–Organization–Resilience" (VOR) framework, for instance, links productivity and metabolism (vigour), structural and functional organization (e.g., biodiversity and network properties), and recovery capacity (resilience) to overall ecosystem condition [2,3,4]. Alongside biological and physico-chemical metrics, integrated indicators have been advocated to synthesize the combined effects of multiple processes on system-level functioning [5]. Thermodynamic indicators are particularly appealing in this context because they connect ecosystem performance to general principles of energy conversion, degradation, and self-organization, and can be evaluated from fluxes and state variables measurable at the canopy scale. Within this thermodynamic perspective, exergy has been proposed as a synthetic measure able to compare disparate flows (radiative, thermal, and chemical) and to quantify irreversibility through exergy destruction [6]. Recent literature emphasizes that exergy-based analysis, necessarily based on a previous energy balance [7,8,9], has progressively expanded into environmental and ecological domains [10], where it has been used to interpret the behaviour of complex, open, non-equilibrium systems and to support sustainability-oriented assessments [11,12].

In ecological applications, exergy-based indicators are attractive because living systems persist far from thermodynamic equilibrium and maintain organized structure by continuously degrading high-quality resources. Jørgensen [13] proposed the use of exergy, structural exergy and ecological buffer capacity as indicators of ecosystem health, relating them to energy flow, conversion efficiency and the maintenance of dynamic equilibria. Other studies presented a Second Law [14] and an exergy analysis of PPS [15,16]. Petela [17] developed an approach to photosynthesis grounded in classical engineering thermodynamics, proposing an exergy balance that jointly accounts for radiation, heat transfer, and matter fluxes across a leaf control volume. Building on a detailed examination of the underlying sub-processes, Silva [18] analysed the exergy flows through photosynthesis to reconcile the wide range of efficiency estimates reported in the literature, identifying the initial absorption of light as the step with the lowest exergy efficiency and as the dominant contributor to overall exergy losses; they reported an overall exergy efficiency of approximately 3.9% under their modelling assumptions. These works support the use of exergy-based indicators to compare photosynthetic performance across conditions, because the Second-Law framing explicitly links useful chemical exergy storage to the degradation of incoming resources.

From an operational perspective, forest health assessment increasingly requires scalable approaches capable of spanning large areas and multi-year time periods, for which sustained *in situ* campaigns are often impractical. Satellite and ancillary meteorological data provide spatially consistent constraints on key drivers and state variables of the canopy system (e.g., incoming radiation, surface temperature, vegetation structure, and albedo), enabling process-based modelling with explicit links to surface–atmosphere exchange.

Recent advances in thermal infrared (TIR) remote sensing make "top-down" thermal information increasingly accessible for ecosystems, supporting thermodynamically consistent accounting and motivating a role for thermal remote sensing ecosystem analysis [19,20,21,22,23,24]. Operational satellite archives routinely provide land surface temperature (LST)—and, in several cases, emissivity—at increasingly useful spatial and

temporal detail, facilitating integration with plot-scale measurements, as documented for MODIS LST products [25] and demonstrated for Sentinel-3 SLSTR operational LST retrieval and validation [26]. Complementary higher-spatial-detail thermal observations are available from Landsat OLI/TIRS [27] and dedicated TIR missions such as ECOSTRESS, which provides atmospherically corrected LST and emissivity products [28]. Together, these developments enable a pragmatic "bottom-up + top-down" strategy in which field measurements identify physiological processes and help defining the proper parameterization, while satellite measurements provide spatially explicit constraints on canopy temperature and longwave exchange—key terms for energy- and exergy budgets [29,30,31,32,33,34,35,36].
In this work we propose a framework for the exergy analysis of PPS in a Mediterranean mixed forest located in the internal coastal area near Roma, Italy, by embedding a lumped representation of photosynthesis within a leaf energy balance model, treating the leaf as an energy converter with coupled radiative, thermal, and biochemical exchanges and neglecting the details of the micro-reactions, as discussed in [17]. Daily averaged datasets combining *in situ* eco-physiological observations (CO_2 and H_2O measured fluxes) [37] and remote sensing products are used to derive exergy-based efficiency indicators at two complementary levels: a system-level indicator that summarizes the overall conversion performance, and a photosynthesis-focused indicator that relates chemical exergy storage to the specific exergy inputs directly involved in the photosynthetic reactions. Together, these indicators are intended to provide quantitative proxies of functional forest condition and to support forest monitoring and sustainable management.

2. Model and Method

2.1. System's mass and energy flows

The system considered in this study is a single leaf treated as an open control volume, exchanging mass and energy with the surrounding environment through radiative, convective, evaporative, and biochemical processes (Figure 1). The photosynthetic reaction is "embedded" in a larger process, customarily referred to as "the leaf light-capturing balance": thus, before addressing directly the PPS "efficiency", it is necessary to analyze in detail the overall mass- and energy balances of this "system leaf". Figure 1a,b,c display a sketch of the mass- and energy in- and outflows on which the balance equations are based. Notice that the fluxes are indicated by explicative names, whereas in the balance equations a more compact notation is adopted. The units are micrograms/(m^2s) for the mass flowrates and W/m^2 for the energy flows, although some experimental inputs are in micromoles/(m^2s) and were accordingly converted.

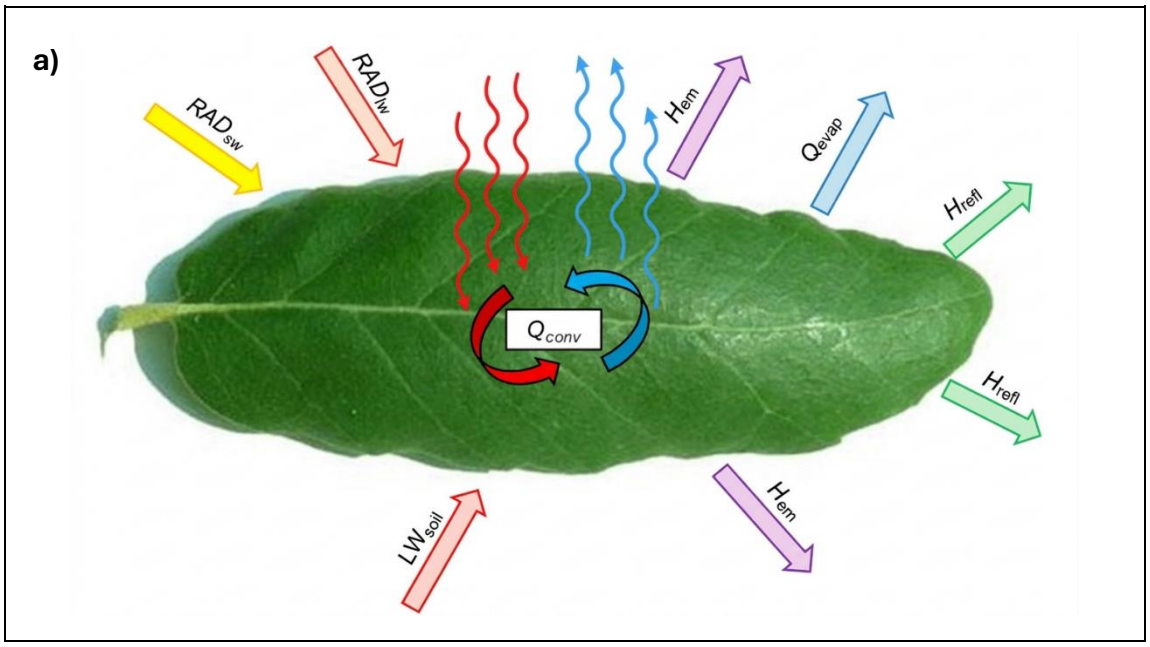

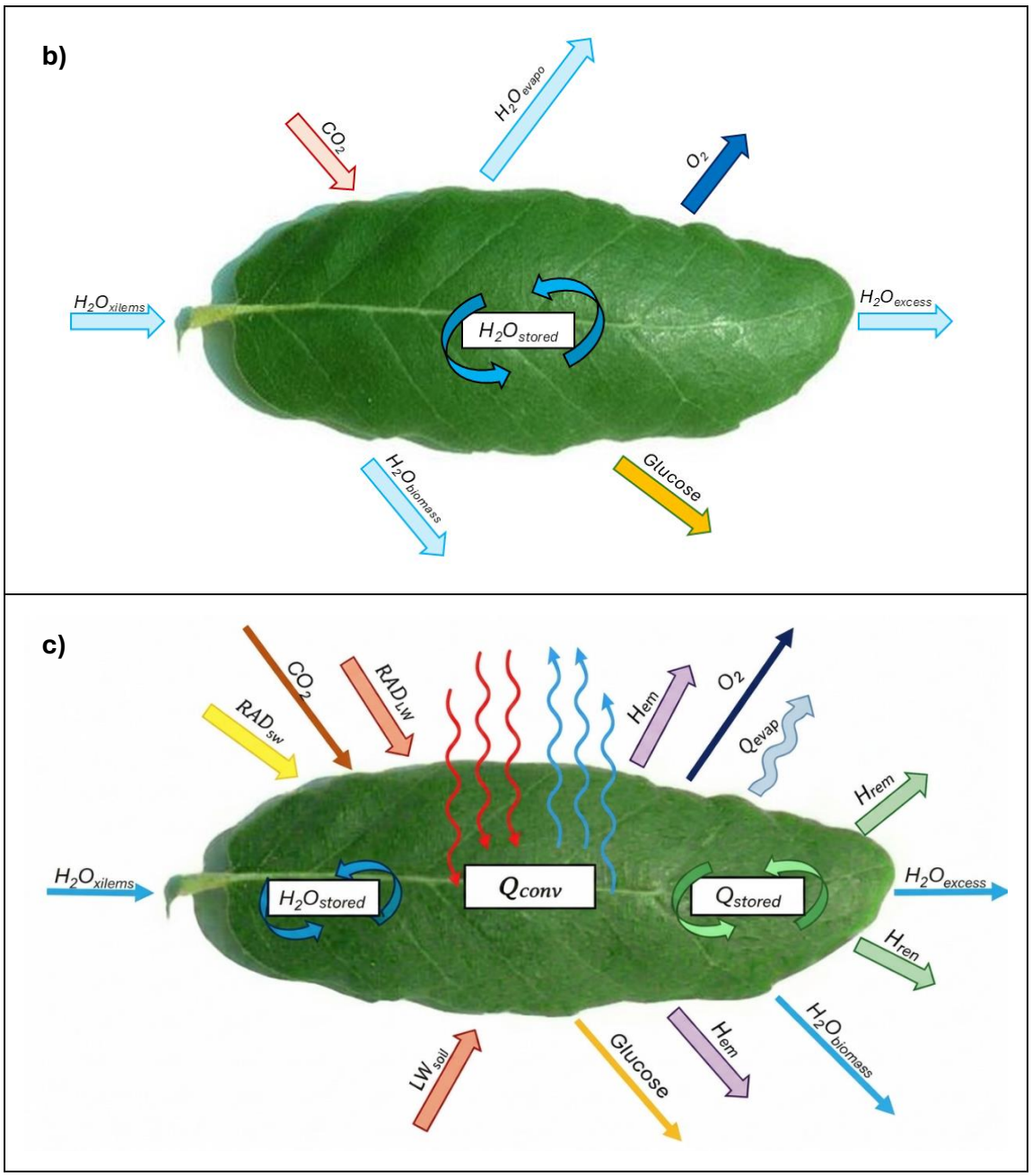

Figure. 1. *Schematic representation of the leaf energy balance* ***(a)****: the leaf exchanges energy with the surrounding environment through absorption of shortwave radiation* (RAD_{SW}) *and longwave radiation/soil* ($RAD_{LW}, SOIL_{LW}$)*, thermal emission* (H_{em})*, latent heat flux associated with evaporation/transpiration* (Q_{evap})*, reflected radiation* (H_{refl})*, and convective heat transfer* (Q_{conv})*. Schematic representation of leaf mass exchange associated with water balance and photosynthetic activity* ***(b)****: water enters the leaf through the xylem* (H_2O_{xylem}) *and is partitioned among internal water storage* (H_2O_{stored})*, structural or biomass-associated water* ($H_2O_{biomass}$)*, evaporative loss as water vapor* (H_2O_{vapor})*, and excess water export* (H_2O_{excess})*. Simultaneously,* CO_2 *is assimilated and converted into glucose, while* O_2 *is released as a by-product of photosynthesis.* ***(c)*** *Schematic overview of coupled leaf energy and mass exchanges, including radiative, convective, and evaporative heat fluxes, xylem water input, internal storage, excess water export, biomass-associated water,* CO_2 *uptake, glucose production, and* O_2 *release.*

2.2. Balance equations and flux parameterization

The water fed to the leaf from the xylemic system is the sole input:

$$m_{w,x} = m_{w,ev} + m_{w,r} + m_{w,nr} \quad (1)$$

And the remaining water flows have their separate sub-balances:

$$m_{w,nr} = m_{w,stor} + m_{w,out} \quad (2)$$

While the reaction water is established by the balance of the PPS reaction ($6CO_2+6H_2O \rightarrow C_6H_{12}O_6+6O_2$):

$$m_{w,r} = \frac{44}{18} m_{CO2} \quad (3)$$

And a separate model [14] is used to calculate the amount of liquid water existing the system with the glucose:

$$m_{w,bio} = 0.1 * \frac{1-Z_{SU}}{Z_{SU}} m_{glucose} \quad (4)$$

With Z_{SU}=0.08 [17].

The energy balance reads:

$$Energy\ Inflow = RAD_{SW} + RAD_{LW} + LW_{soil} + H_{CO2} + H_{w,x}$$

$$Energy\ Outflow = H_{refl} + H_{em} + Q_{evap} + Q_{stored} + H_{evap} + H_{O2} + H_{w,bio} + H_{glucose} + H_{w,out}$$

This is a dynamic balance that is closed at each instant of time by an accumulation term:

$$\Delta H_{structure} = H_{in} - H_{out} \quad (5)$$

Notice the difference between the terms Q_{stored} and $\Delta E_{structure}$: the first represents the sensible heat increase (or decrease) due to the variation of the leaf temperature:

$$Q_{stored} = c_{p,leaf} \rho_{leaf} V_{leaf} \Delta T_{leaf} \quad (6)$$

While the second is the total gain -or loss of thermal energy caused by the irradiation and environmental conditions; in the present model, this term is interpreted as thermal storage because the chemical contribution of photosynthesis is already accounted for separately through the reactant and product terms.

Shortwave radiation (RAD_{SW}) and photosynthetically active radiation (PAR) were provided by the "Ladispoli Palo-Laziale" meteorological station, located within the study site and operated by the Agrometeorological Service of the Lazio Region (SIARL) [38] since 2018 Longwave radiation (RAD_{LW}) was derived from the NASA POWER dataset [39].

The soil longwave radiation LW_{soil} and the leaf thermal re-radiation E_{em} are calculated as:

$$LW_{soil} = \varepsilon_{soil} \sigma_B T_{soil}^4 \quad (7)$$

$$H_{em} = f_{em} \varepsilon_{leaf} \sigma_B T_{leaf}^4 \quad (8)$$

Where f_{em} is a factor between 1 and 2 that accounts for the possible local shading ("view factor": the leaf emits from both sides, but neighboring leaves may shade portions of the thermal rays).

Soil temperature (T_{soil}) was measured in situ using a probe installed within the study area at a depth of 30 cm. Leaf temperature (T_{leaf}) was estimated from Land Surface Temperature (LST) from Landsat 8 Collection 2 Level 2 imagery acquired over the 2018–2022 period [40]. The resulting LST values were matched with the corresponding recorded air temperature (T_{air}) values, and an empirical relationship was derived to estimate leaf temperature on a daily basis over the window of observation ($T_{leaf} = 1.34 * T_{air}$).

The leaf shortwave reflection H_{refl} is calculated as:

$$H_{refl} = f_{refl}[r_{SW} RAD_{SW} + r_{LW}(RAD_{LW} + LW_{soil})] \quad (9)$$

With r_{SW} and r_{LW} are the average leaf reflectance in the respective spectra.

Net radiation is calculated by the so-called Okajima formulae [41]:

$$RAD_{net} = \alpha_{SW}(1 + alb_{SW}) RAD_{SW} + \alpha_{LW}(LW + LW_{soil}) - H_{em} - H_{refl} \quad (10)$$

The mass flow rates of CO_2 and evaporated H_2O were derived from molar flow rates measured with a portable infrared gas exchange analyser, Ciras-2 (Portable Photosynthesis System, © 2010 PP Systems). Leaf gas-exchange measurements were performed using a spot-measurement approach, consisting of instantaneous snapshots of physiological parameters under the prevailing environmental conditions. These measured values were further used to calibrate and validate the MOCA model, a deterministic semi-empirical process-based model able to simulate the main eco-physiological parameters at the daily scale over the study years, including CO_2 assimilation, stomatal conductance, and evapotranspiration, based on climatic inputs and species-specific parameters [34].

$$m_{CO2} = 44 n_{CO2}\ ; \qquad m_{w,evap} = 18 n_{w,evap} \quad (11)$$

The enthalpy of the water, of the CO_2 and of the O_2 are calculated as a function of the temperature using the minRefProp application [42] (the assumption being that the flows are at atmospheric pressure). For glucose, the standard molar enthalpy of formation was taken from the NIST Chemistry WebBook [43]. The enthalpy change of evaporation is also calculated from minRefProp by assuming that the water evaporates at p_{atm} and T_{leaf}.

The convection loss (or gain) Q_{conv} is calculated from:

$$Q_{conv} = h_{conv} A_{leaf} (T_{leaf} - T_{air}) \quad (12)$$

With $h_{conv} = 2.8 + 3 * f_{wind} V_{wind}$, where f_{wind}<1 is an average intensity correction factor through the canopy and V_{wind} is the top-of-the-canopy velocity measured by the Palo Laziale meteorological station.

The fraction of the APAR that is actually feeding the PPS reaction and determines the biomass generation ($m_{glucose}$+$m_{w,bio}$) is calculated via the Beer-Lambert formula [22]:

$$fAPAR = 1 - \exp[-k_{BL} LAI] \quad (13)$$

Where LAI is the Leaf Area Index, measured in the field using an LAI-2000 Plant Canopy Analyzer (LI-COR Biosciences), and subsequently estimated at the daily scale through a site-calibrated relationship with the Normalized Difference Vegetation Index (NDVI) [37]. In turn, $k_{BL}$was calculated as a function of LAI as [37,44]:

$$k_{BL} = \frac{0.91 * LAI}{(0.54 + LAI)} \quad (14)$$

The *APAR* is obtained by multiplying *PAR* by *fAPAR*:

$$APAR = fAPAR * PAR \quad (15)$$

2.3. The exergy budget

For material flows, the exergy was calculated as:

$$E_j = m_j e_j$$

Where the e_j is the specific exergies of the *j-th* material.
For thermal flows (convection, stored heat), the exergy was calculated as:

$$E_{Qj} = Q_j f_{C,j}$$

Where the $f_{Q,j}$ is the relevant Carnot factor ($1-T_j/T_0$) of the *j-th* energy flow.
For radiation flows, the exergy was calculated as:

$$E_{Ij} = I_j f_{P,j}$$

Where the f_{Pj} is the Petela exergy conversion factor for the *j-th* LW or SW radiation flow [17].
Exergy being a non-conserved quantity, the difference between the cumulative exergy input and the sum of the outputs is always positive and equal to a virtual quantity called the exergy destruction, E_δ that represents the destruction of useful energy in the process. The Second Law efficiencies were calculated as the ratio of the useful outputs to the cumulative input.

3. Results

The collected dataset consists of 5 years (2018-2022) of daily measurements. For each year, one "typical" winter and summer days were selected, and the results of the model instantiation are reported in Table 1.

***Table. 1**. Model results for selected winter and summer days for each year. Values in red are the results of the simulation.*

2018	***Winter***	***Summer***	***2019***	***Winter***	***Summer***
RAD	*163*	*450*	**RAD**	*284*	*559*
PAR	*81*	*210*	**PAR**	*142*	*182*
T_{air}	*283*	*295*	***T_{air}***	*283*	*297*
T_{water}	*283*	*295*	**T_{water}**	*283*	*298*
T_{leaf}	*287*	*296*	**T_{leaf}**	*288*	*303*
T_{soil}	*280*	*294*	**T_{soil}**	*282*	*295*
µmol CO_2	*1.088*	*4.959*	**µmol CO_2**	*1.390*	*4.586*
µmol H_2O_{ev}	*1155*	*7449*	**µmol H_2O_{ev}**	*2404*	*6012*
V_{wind}	*3.280*	*3.570*	***V_{wind}***	*5.000*	*4.100*
LAI	*2.810*	*3.160*	***LAI***	*2.910*	*3.160*
$\Delta H_{stored}/H_{tot,in}$	**0.128**	**0.0238**	***$\Delta H_{stored}/H_{tot,in}$***	**0.0186**	**0.127**
$\eta_{2,system}$	**0.0247**	**0.0145**	***$\eta_{2,system}$***	**0.018**	**0.0074**
$\eta_{2,PPS}$	**0.0355**	**0.021**	***$\eta_{2,PPS}$***	**0.024**	**0.014**
2020	***Winter***	***Summer***	***2021***	***Winter***	***Summer***
RAD	*433*	*544*	**RAD**	*289*	*490*
PAR	*210*	*154*	**PAR**	*134*	*235*
T_{air}	*285*	*297*	**T_{air}**	*281*	*298*
T_{water}	*285*	*297*	**T_{water}**	*281*	*298*
T_{leaf}	*293*	*305*	**T_{leaf}**	*288*	*306*
T_{soil}	*281*	*295*	**T_{soil}**	*284*	*299*
µmol CO_2	*2.682*	*3.039*	**µmol CO_2**	*1.308*	*4.965*
µmol H_2O_{ev}	*2586*	*5618*	**µmol H_2O_{ev}**	*2031*	*4915*

V_{wind}	3.100	4.000	V_{wind}	3.400	4.600
LAI	3.060	3.060	LAI	2.940	3.120
$\Delta H_{stored}/H_{tot,in}$	0.12	0.085	$\Delta H_{stored}/H_{tot,in}$	0.086	0.065
$\eta_{2,system}$	0.012	0.0076	$\eta_{2,system}$	0.0184	0.012
$\eta_{2,PPS}$	0.02	0.011	$\eta_{2,PPS}$	0.0238	0.012

2022	Winter	Summer
RAD	230	560
PAR	111	182
T_{air}	282	298
T_{water}	282	298
T_{leaf}	285	306
T_{soil}	284	285
µmol CO_2	1.117	3.137
µmol H_2O_{ev}	2656	4750
V_{wind}	6.200	3.100
LAI	3.110	3.060
$\Delta H_{stored}/H_{tot,in}$	0.053	0.184
$\eta_{2,system}$	0.023	0.008
$\eta_{2,PPS}$	0.0293	0.0999

3.1. Photosynthetic Energy and Exergy Efficiency

To provide an interpretation of the thermodynamic behavior of photosynthesis, a representative summer case was selected from the 2020 study period. The set of input variables used for the calculations is summarized in Table 2. This reference case provides an intuitive framework for discussing how energy and exergy are partitioned among the different terms involved in the stoichiometric photosynthetic reaction (Figure.2a, b).

Table. 2. *Environmental and physiological input variables adopted for the representative summer 2020 case used in the energy and exergy analysis of the leaf photosynthetic system. Radiation terms (RAD and PAR) are expressed in W/m²; temperatures in K; CO_2 assimilation and H_2O evaporation fluxes in µmol/(m² s); wind velocity in m/s; and Leaf Area Index (LAI) in m²leaf /m²soil. The temperature of the water entering the leaf was assumed to be equal to air temperature [45].*

2020	RAD	PAR	T_{air}	T_{water}	T_{leaf}	T_{soil}	CO_2	H_2O_{evap}	V_{wind}	LAI
Summer	554	154	297	297	305	295	3.04	5618	4.00	3.06

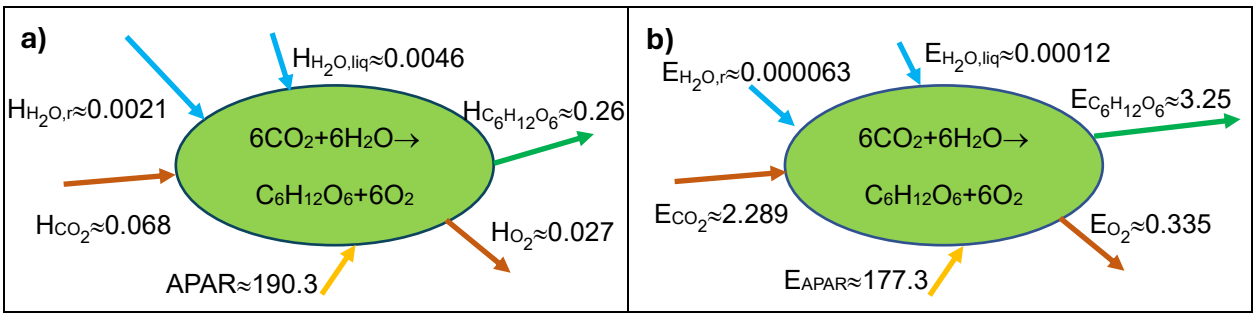

Figure. 2. *"Typical" (summer 2020) energy* ***(a)*** *&* *exergy* ***(b)*** *flows for the stoichiometric photosynthesis reaction, W/m²leaf.*

It is clear that the major input is the *APAR* radiation, but it is interesting to examine the remaining flows: the energy inputs are of the order of 10^{-3} to 10^{-4} of the *APAR*, and thus the energy efficiency of the process, calculated as the ratio

$$\eta_{1,PPS} = \frac{H_{C6H12O6}+H_{O2}}{APAR+\sum(H_{inputs})} \quad (16)$$

is of the same order (namely 0.0014).

The exergy budget shows a different picture: while the exergy of the *APAR* (equal to *APAR* multiplied by approximately 0.93 the Petela factor) is still rather high, the exergy of the glucose and of the CO_2 is between 2 and 3% of the E_{APAR}, while the exergy of the remaining terms, especially of the H_2O, is quite low, since the water is at the leaf temperature. This causes the exergetic efficiency $\eta_{2,PPS} = \frac{E_{C6H12O6}+E_{O2}}{E_{APAR}+\sum(E_{inputs})} = 0.02$ to be higher than its energy counterpart. Notice that the exergy destruction in the reaction is very high:

$$E_{\delta,PPS} = \sum(E_{inputs}) - \sum(E_{outputs}) \cong 176 \quad \text{W/m}^2_{\text{leaf}}, \text{ i.e., about 99\%.}$$

The above results offer some additional insight into the physics of the process: to generate the sap needed for the plant's growth, the process exploits a high exergy (=low entropy) flow to enact a chemical transformation of an atmospheric gas (CO_2) into a complex molecule (glucose). The O_2 that in an anthropic perspective is regarded as "beneficial" is just a byproduct required by the chemical balance, and the remaining flows are only necessary complements to the maintenance of the reaction.

3.2. Sensitivity to process parameters

To assess the congruence of the model, a sensitivity analysis was conducted on the 5 selected days of year 2020. The varied parameters were LAI, n_{evap,H_2O}, RAD_{SW}, T_{soil} and T_{leaf} and the control outputs the ΔH_{stored}, $\eta_{1,PPS}$ and $\eta_{2,PPS}$ The results are quite interesting:

a) The *LAI* effect is almost negligible, except for a slight variation of the E_{destr}. This is due to the reduced influence that the *LAI* has on the *fAPAR* (eq. 13): the variation in the ΔH_{stored} and in both $\eta_{1,PPS}$ and $\eta_{2,PPS}$ are less than a few percentage points.

b) Also the variation (±10%) of the moles of evapotranspirated water causes a slight and almost linear increase in both η_2 and $\eta_{2,PPS}$ and a corresponding decrease in ΔH_{stored}. The reason lies in the fact that the total water influx from the xylems, m_{wx}, is proportional to the sum of $m_{evap}+m_{wr}$ (eqs. 1 & 2), and thus the reaction water remains the same and only the non-reacting water (of very low energy & exergy) is affected. ΔH_{stored} decreases because, *ceteris paribus*, the energy/exergy outflow increases with m_{evap}.

c) A ±10% variation of the RAD_{SW} leads to a linear decrease in ΔH_{stored} due to an "overcompensation" caused by the reflected radiation and the leaf re-emission. It barely affects the remaining parameters, except for a slight increase in η_2 due to an actual reduction of the *APAR*.

d) A ±3 K variation of T_{soil} is reflected in a slight quadratic increase of ΔH_{stored}, due to the non-negligible contribution of the soil RAD_{LW}.

e) T_{leaf} is the parameter that influences the most the model output. A ±3 K variation causes a decrease in ΔH_{stored} due to the leaf re-radiation and to the increased convection Q_{conv}: in extreme cases (+3K), the storage is negative, meaning that the plant actually releases energy to the environment. In winter, both η_2 and $\eta_{2,PPS}$ decrease with T_{leaf}, while in summer the higher RAD_{SW} compensates for the re-emission and convection and η_2 increases quadratically. Figure 3 displays these results.

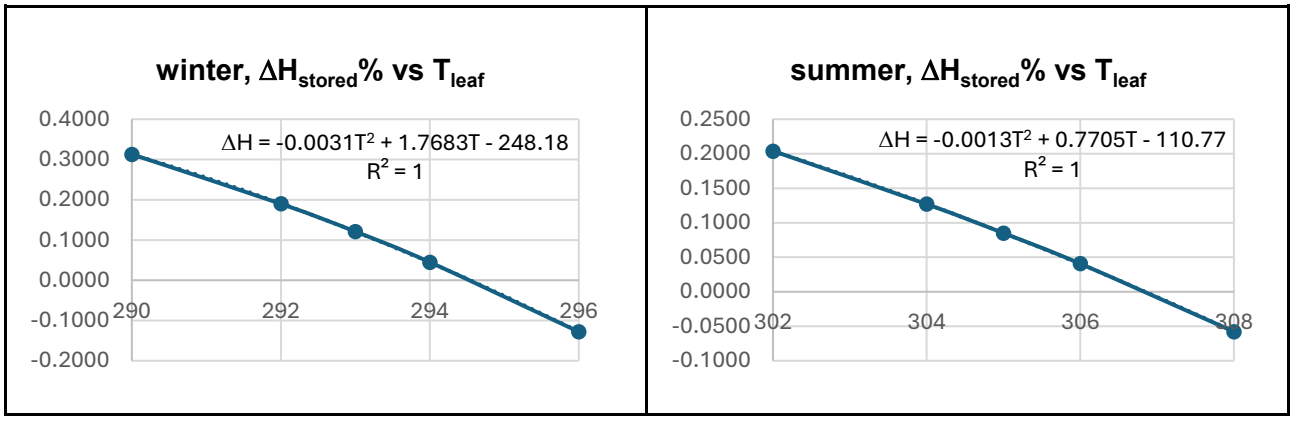

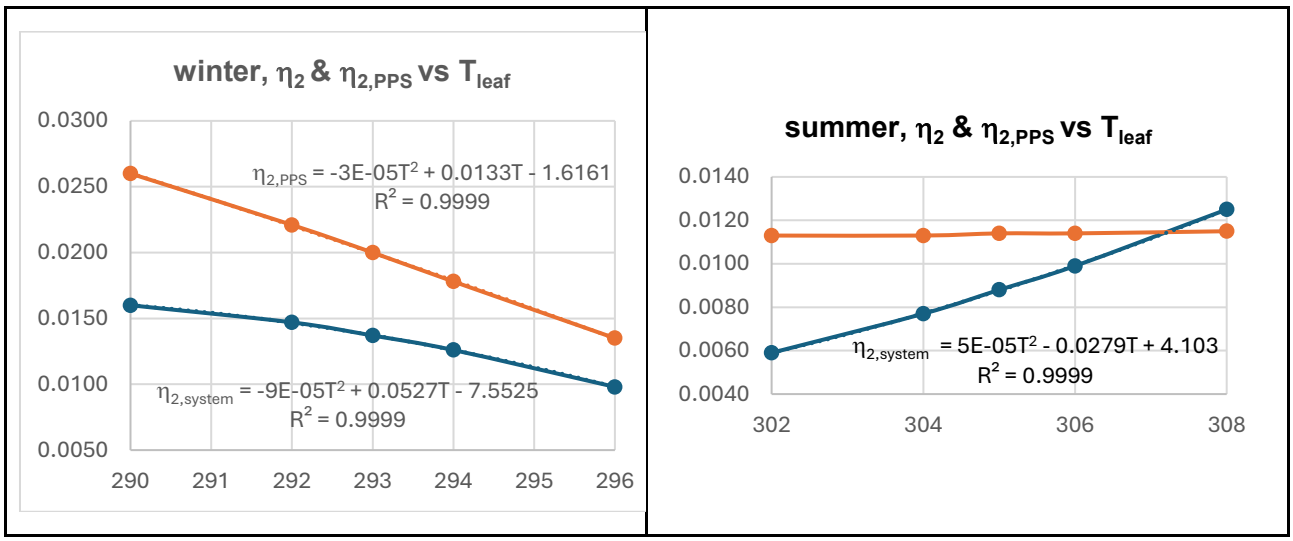

Figure. 3. *Sensitivity of ΔH_{stored}, η_2 and $\eta_{2,PPS}$ to variations of T_{leaf}.*

4. Conclusions

A lumped model (at leaf level) of the photosynthesis conversion is proposed in this paper. Mass- and energy balances are extensively based on satellite data, substantially reducing the number of empirical correlations used in similar studies. The model is applied to a very large database of 5 years' worth of measurements, and from the balances an exergy analysis is performed. The results indicate that while from a First Law approach the leaf stores between 0.01 and 0.12 of the total energy input, when it is regarded as an "exergy converter" has a Second Law efficiency quite sensitive to seasonal variations but always contained in the range $0.006<h_{2,leaf}<0.02$ (implying that the process destroys between 98% and 99.4% of the incoming exergy). The lumped balance of the PPS reaction indicates that its efficiency also varies throughout the seasons, with values between 0.01 and 0.08, with an exergy destruction of 92-99%. The overall conversion from the material and energy inputs (water, CO_2, LW and SW radiation) to the useful outputs (glucose, leaf hydration, O_2) is quite high (0.01 to 0.13). The system displays a high degree of self-regulation and the sensitivity of the results to several environmental parameters (RAD_{LW}, T_{soil}, T_{air}) is surprisingly low. The most influential parameter is T_{leaf}, because of its effects on leaf absorption and re-radiation in the LW spectrum. Future developments of this work will focus, first, on the application of the model to measured data from eddy covariance towers of the ICOS and FLUXNET networks, with the aim of providing a first large-scale quantification of forest thermodynamic efficiency across different biomes and environmental conditions. In parallel, a spatially explicit methodology will be developed to fully exploit satellite observations and estimate forest efficiency also in areas lacking direct measurements.

Acknowledgments

DL and MV would like to acknowledge the LIFE PRIMED project (LIFE17 NAT/GR/000511 - Restoration, management, and valorisation of PRIority habitats of MEDiterranean coastal areas), Oasi WWF Bosco di Palo, and the Integrated Agrometeorological Service of the Lazio Region (SIARL). They also wish to thank all the people who contributed to the LIFE PRIMED project, with special thanks to Dr. Kristina Micalizzi and Dr. Francesca Ferroni for their commitment and valuable support in the collection of field data.

Nomenclature

$APAR$ Absorbed Photosynthetically Active Radiation, W/m^2

H_{em} Leaf Re-Radiation Energy, W/m^2

H_{refl} Leaf Energy Reflected, W/m^2

$fAPAR$ Fraction of Absorbed Photosynthetically Active Radiation, W/m^2

LW_{soil} Soil Long-Wave Radiation, W/m^2

$m_{w,x}$ Water entering the leaf, μg/(m^{2}s)

$m_{w,ev}$ Water evapotraspirated, μg/(m^{2}s)

$m_{w,r}$ Reaction Water in Photosynthesis process, μg/(m^{2}s)

$m_{w,nr}$ Non-Reaction Water, μg/(m^{2}s)

$m_{w,stor}$ Water stored, μg/(m^{2}s), μg/(m^{2}s)

$m_{w,bio}$ Water within the generated biomass, μg/(m²s)

$m_{glucose}$ Amount of produced Sugar, μg/(m²s)

m_{CO2} CO_2 absorbed, μg/(m²s)

m_{O2} O_2 relased, μg/(m²s)

PAR Photosynthetically Active Radiation, W/m²

Q_{conv} Sensible Heat between Leaf and Atmosphere, W/m²

Q_{evap} Latent Heat of Evapotranspiration, W/m²

RAD_{LW} Long-Wave Radiation Absorbed Dose, W/m²

RAD_{SW} Short-Wave Radiation Absorbed Dose, W/m²

Z_{su} Mole fraction of sugar in the biomass, adimensional

References

[1] Silow EA, Mokry AV, Jørgensen SE. Eco-exergy use for ecosystem health assessment. In: International Journal of Exergy. Paris; 2011.

[2] Costanza R. Toward an operational definition of ecosystem health. In: Ecosystem Health: New Goals for Environmental Management. 1992:239-269.

[3] Rapport DJ, Costanza R, McMichael AJ. Assessing ecosystem health. Trends Ecol Evol 1998;13:397-402.

[4] Lu Y, Wang R, Zhang Y, Su H, Wang P, Jenkins A, Ferrier RC, Bailey M, Squire G. Ecosystem health towards sustainability. Ecosyst Health Sustain 2015;1:1-15.

[5] Jørgensen SE. Evolutionary essays: A thermodynamic interpretation of the evolution. Oxford: Elsevier; 2011.

[6] Moran MJ, Sciubba E. Exergy analysis: Principles and practice. J Eng Gas Turbines Power 1994;116(2):285-290.

[7] Albarrán-Zavala E, Angulo-Brown F. A simple thermodynamic analysis of photosynthesis. Entropy 2007;9:152-168.

[8] Arkebauer TJ. Leaf radiative properties and the leaf energy budget. Agron Hortic Fac Publ 2005;693. https://digitalcommons.unl.edu/agronomyfacpub/693

[9] Muir CD. tealeaves: An R package for modelling leaf temperature using energy budgets. AoB PLANTS 2019;11.

[10] Attorre F, Sciubba E, Vitale M. A thermodynamic model for plant growth, validated with Pinus sylvestris data. Ecol Modell 2019;391:53-62.

[11] Alzaben H, Fraser R. Energy and exergy analyses applied to a crop plant system. Thermo 2025;5(1):3.

[12] Dewulf J, Van Langenhove H, Muys B, Bruers S, Bakshi BR, Grubb GF, Paulus DM, Sciubba E. Exergy: Its potential and limitations in environmental science and technology. Environ Sci Technol 2008;42(7):2221-2232.

[13] Jørgensen SE, Nielsen SN, Mejer H. Emergy, environ, exergy and ecological modelling. Ecol Modell 1995;77:99-109.

[14] Bisio G, Bisio A. Thermodynamic analysis of photosynthesis. In: Proceedings of the 29th Intersociety Energy Conversion Engineering Conference. Monterey, CA, USA; 1994. p. 323-328.

[15] Grishin AP, Grishin AA, Grishin VA. Methods for determining exergy photosynthesis in crop production. IOP Conf Ser Earth Environ Sci 2021;839(4):042001.

[16] Lems S, Van Der Kooi HJ, De Swaan Arons J. Exergy analyses of the biochemical processes of photosynthesis. Int J Exergy 2010;7(3):333-351.

[17] Petela R. An approach to the exergy analysis of photosynthesis. Sol Energy 2008;82:311-328.

[18] Silva CS, Seider WD, Lior N. Exergy efficiency of plant photosynthesis. Chem Eng Sci 2015.

[19] Choudhury BJ. Estimating gross photosynthesis using satellite and ancillary data: Approach and preliminary results. Remote Sens Environ 2001;75:1-21.

[20] Ganz S, Adler P, Kändler G. Forest cover mapping based on a combination of aerial images and Sentinel-2 satellite data compared to national forest inventory data. Forests 2020;11.

[21] Guimarães N, Pádua L, Marques P, Silva N, Peres E, Sousa JJ. Forestry remote sensing from unmanned aerial vehicles: A review focusing on the data, processing and potentialities. Remote Sens 2020;12:1046.

[22] Li R, Li B, Yuan Y, Liu W, Zhu J, Qi J, Tan Q. Improvement of FAPAR estimation under the presence of non-green vegetation considering fractional vegetation coverage. Remote Sens 2025;17(4):603.

[23] Luvall JC, Rickman D, Fraser RF. Thermal remote sensing and the thermodynamics of ecosystem development. NASA Technical Reports Server, presentation/report no. M14-3592; 2014.

[24] Fraser RA, Kay JJ. Exergy analysis of ecosystems: Establishing a role for thermal remote sensing. In: Thermal remote sensing in land surface processing. Boca Raton: CRC Press; 2004. p. 283-360.

[25] Wan Z. New refinements and validation of the Collection-6 MODIS land-surface temperature/emissivity product. Remote Sens Environ 2014;140:36-45.
[26] Pérez-Planells L, Niclòs R, Valiente JA, Coll C, Sánchez JM, Galve JM, et al. Validation of Sentinel-3 SLSTR land surface temperature retrieved by the operational product and comparison with explicitly emissivity-dependent algorithms. Remote Sens 2021;13(11):2228.
[27] Earth Resources Observation and Science Center. Landsat 8-9 Operational Land Imager / Thermal Infrared Sensor Level-2, Collection 2 [dataset]. U.S. Geological Survey; 2020.
[28] Meerdink SK, Hook SJ, Roberts DA, Abbott EA. The ECOSTRESS spectral library version 1.0. Remote Sens Environ 2019;230:111196.
[29] Badgley G, Field CB, Berry JA. Canopy near-infrared reflectance and terrestrial photosynthesis. Sci Adv 2017;3(3):e1602244.
[30] Gutschick VP. Leaf energy balance: Basics, and modeling from leaves to canopies. In: Hikosaka K, Niinemets U, Anten NPR, editors. Canopy photosynthesis: From basics to applications. 2015.
[31] Moon K, Duff TJ, Tolhurst KG. Characterising forest wind profiles for utilisation in fire spread models. In: 20th International Congress on Modelling & Simulation. Adelaide, Australia; 1-6 December 2013.
[32] Paul KI, Polglase PJ, Smethurst PJ, O'Connell AM, Carlyle CJ, Khanna PK. Soil temperature under forests: A simple model for predicting soil temperature under a range of forest types. Agric For Meteorol 2004;121:167-182.
[33] Wang XC, Wang CK, Li QL. Wind regimes above and below a temperate deciduous forest canopy in complex terrain: Interactions between slope and valley winds. Atmosphere 2015;6:60.
[34] Xu CY, Qu JJ, Hao XJ, Zhu ZL, Gutenberg L. Surface soil temperature seasonal variation estimation in a forested area using combined satellite observations and in-situ measurements. Int J Appl Earth Obs Geoinf 2020;91:102156.
[35] Quattrochi DA, Luvall JC. Thermal infrared remote sensing for analysis of landscape ecological processes: Methods and applications. Landsc Ecol 1999;14(6):577-598.
[36] Luvall JC, Rickman DL, Arnold JE. The use of thermal remote sensing to study thermodynamics of ecosystem development. In: Multi/Hyperspectral Sensors, Measurements, Modeling and Simulation. January 2000.
[37] Lombardi D, Micalizzi K, Vitale M. Assessing carbon and water fluxes in a mixed Mediterranean protected forest under climate change: An integrated bottom-up and top-down approach. Ecol Inform 2023;78:102318.
[38] SIARL Lazio. Available from: https://www.siarl-lazio.it/. Accessed December 2025.
[39] NASA POWER. Available from: https://power.larc.nasa.gov/. Accessed December 2025.
[40] Ermida SL, Soares P, Mantas V, Göttsche FM, Trigo IF. Google Earth Engine open-source code for land surface temperature estimation from the Landsat series. Remote Sens 2020;12(9):1471.
[41] Okajima Y, Taneda H, Noguchi K, Terashima I. Optimum leaf size predicted by a novel leaf energy balance model incorporating dependencies of photosynthesis on light and temperature. Ecol Res 2012;27:333-346.
[42] Lemmon EW, Bell IH, Huber ML, McLinden MO. NIST Standard Reference Database 23: Reference Fluid Thermodynamic and Transport Properties—REFPROP, version 10.0. Gaithersburg: NIST Standard Reference Data Program; 2018.
[43] Linstrom PJ, Mallard WG. The NIST Chemistry WebBook: A chemical data resource on the internet. J Chem Eng Data 2001;46(5):1059-1063.
[44] Vitale M, Scimone M, Feoli E, Manes F. Modelling leaf gas exchanges to predict functional trends in Mediterranean Quercus ilex forest under climatic changes in temperature. Ecol Modell 2003;166:123-134.
[45] Román-Écija M, Landa BB, Testi L, Navas-Cortés JA. Thermal dynamics of xylem and soil-root temperatures in olive and almond trees and their relationship with air temperature. Agronomy 2025;16(1):102.